

Limits to velocity of signal propagation in many-body systems: a quantum-information perspective

Piotr Wysocki and Jan Chwedeńczuk*

Faculty of Physics, University of Warsaw, ul. Pasteura 5, 02-093 Warszawa, Poland

The Lieb-Robinson bound (LRB) states that the range and strength of interactions between the constituents of a complex many-body system impose upper limits to how fast the signal can propagate. It manifests in a light cone-like growth of correlation function connecting two distant subsystems. Here we employ the techniques of quantum information to demonstrate that the LRB can be determined from local measurements performed on a single qubit that is connected to a many-body system. This formulation provides an operational recipe for estimating the LRB in complex systems, replacing the measurement of the correlation function with simple single-particle manipulations. We demonstrate the potency of this approach by deriving the upper limit to the speed of signal propagation in the XY spin chain.

The Lieb-Robinson bound imposes an upper limit to the speed of signal propagation in quantum systems [1]. It is quantified by considering two systems, A and B , distanced by d and evolving according to some Hamiltonian \hat{H} . The LRB states that the norm of the commutator $[\hat{A}, \hat{B}(t)]$ is bounded by

$$\|[\hat{A}, \hat{B}(t)]\| \leq a e^{-(d-vt)}, \quad (1)$$

where a depends on the operators \hat{A} , $\hat{B}(t)$ and the Hamiltonian, while the propagation speed v is determined solely by the details of \hat{H} . In the wake of the discovery of this fundamental relation, vast experimental and theoretical effort was invested into measuring or calculating this bound for various systems. The LRB is very important for the development of quantum technologies, as it governs the information spreading across quantum circuits [2–8], and its role has been recognized as a limiting factor to the performance of quantum heat engines [9]. It is also an important probe of the microscopic properties of many-body quantum systems [10–12]. It is a determinant of correlations strength build-up in complex systems [13–17], a quantity that is directly measurable in experiment [18]. Recently it has been shown that the LRB influences the rate of entanglement growth in many-body systems [19, 20].

Usually, the LRB is obtained from the measurement of the correlation function between the two distant subsystems. We propose a different route, and show that the LRB can be determined with simple local measurements on a single qubit that is connected to a many-body system. This stems from the observation that the amount of information about the initial perturbation applied to some part of the system distant from the qubit, which propagates under a Hamiltonian \hat{H} , is inherently bounded by the LRB. This result is obtained using the tool known as the quantum Fisher information

(QFI) [21]. Although it is usually invoked in the context of quantum metrology, as it sets the lower bound to the sensitivity of quantum sensors [22], the QFI is a versatile tool, allowing to determine the strength of multipartite entanglement [23–25], the Einstein-Podolsky-Rosen steering [26], or the Bell nonlocality [27]. It is also a fine probe of quantum- and thermal-phase transitions in complex systems [25, 28–37]. Here, the QFI again proves to be a potent tool, opening a way towards simple determination of the LRB in many-body systems.

The process, illustrated in Fig. 1, starts with an impulse that acts for time τ on some subsystem that becomes a *source* of the signal. This first step can be expressed as

$$\hat{\rho}(\theta) = e^{-i\theta\hat{H}_{sr}} \hat{\rho} e^{i\theta\hat{H}_{sr}}, \quad (2)$$

where $\hat{\rho}$ is the initial density operator of the full system and \hat{H}_{sr} is the (local) source Hamiltonian. The parameter $\theta = \omega\tau$ is the measure of the coupling strength to the external potential and ω is some characteristic frequency.

Subsequently, a Hamiltonian \hat{H} triggers the propagation of the signal across the system, yielding the outcome

$$\hat{\rho}(\theta; t) = e^{-it\hat{H}} \hat{\rho}(\theta) e^{it\hat{H}}. \quad (3)$$

The main question of this work can be stated as follows: how fast does the information about θ , the parameter connected to the triggering impulse, propagate to the *receiver*—a subsystem distant from the source?

We provide an answer making a single assumption: the receiver is a single qubit with its local density operator

$$\hat{\rho}_{rc}^{(\theta)}(t) = \widetilde{\text{Tr}}[\hat{\rho}(\theta; t)], \quad (4)$$

where the tilde denotes the partial trace over all the non-receiver degrees of freedom.

The information about the impulse that can be extracted from any measurements on the receiver is no larger than the QFI, which is denoted by $\mathcal{I}_{rc}^{(q)}$ and has

* jan.chwedenczuk@fuw.edu.pl



FIG. 1. Illustration showing the source (dark blue square) sending the signal through the many-body system to the single receiving qubit. The LRB is derived from the single-particle local operations.

a general form of

$$\mathcal{I}_{rc}^{(q)} = 2 \sum_{i \neq j} \frac{|\langle \psi_j | \dot{\hat{\rho}}_{rc}^{(\theta)}(t) | \psi_i \rangle|^2}{p_i + p_j}, \quad (5)$$

where the summation runs over the elements of the spectrum of $\hat{\rho}_{rc}^{(\theta)}(t)$, $|\psi_{i/j}\rangle$ are its eigenstates and $p_{i/j}$ the corresponding eigenvalues. The dot denotes the derivative of the density operator with respect to the parameter θ . For a receiver that is a qubit with two eigenstates and probabilities that add to unity, this reduces to

$$\mathcal{I}_{rc}^{(q)} = 4 |\langle \psi_1 | \dot{\hat{\rho}}_{rc}^{(\theta)}(t) | \psi_2 \rangle|^2 = 4 |\text{Tr}[\hat{\sigma}_- \dot{\hat{\rho}}(\theta, t)]|^2, \quad (6)$$

where $\hat{\sigma}_- = |\psi_1\rangle\langle\psi_2|$ and the trace now runs over the Hilbert space of the whole system. The $\mathcal{I}_{rc}^{(q)}$ is a convex functional of the density operator [22], hence by using the spectral decomposition of the density matrix $\hat{\rho}(\theta) = \sum_n p_n |\Psi_n\rangle\langle\Psi_n|$ and Eq. (2), we obtain

$$\begin{aligned} \mathcal{I}_{rc}^{(q)} &= 4 |\text{Tr}[\hat{\sigma}_- e^{-it\hat{H}} [\hat{H}_{sr}, \sum_n p_n |\Psi_n\rangle\langle\Psi_n|] e^{it\hat{H}}]|^2 \\ &\leq 4 \sum_n p_n |\text{Tr}[\hat{\sigma}_-(t) [\hat{H}_{sr}, |\Psi_n\rangle\langle\Psi_n|]]|^2, \end{aligned} \quad (7)$$

where $\hat{\sigma}_-(t) = e^{it\hat{H}} \hat{\sigma}_- e^{-it\hat{H}}$. The trace can be calculated using the basis of $|\Psi_n\rangle$'s, giving

$$\mathcal{I}_{rc}^{(q)} \leq 4 \sum_n p_n |\langle \Psi_n | [\hat{\sigma}_-(t), \hat{H}_{sr}] | \Psi_n \rangle|^2. \quad (8)$$

The emergent commutator $\hat{\mathcal{C}}(t) \equiv [\hat{\sigma}_-(t), \hat{H}_{sr}]$ of operators related to the source and receiver (at time t) subsystems is the quantity that is at the core of the original Lieb-Robinson analysis [1], see Eq. (1). The final step is to note that

$$\begin{aligned} |\langle \Psi_n | \hat{\mathcal{C}}(t) | \Psi_n \rangle|^2 &= \langle \Psi_n | \hat{\mathcal{C}}^\dagger(t) (\hat{\mathbb{1}} - \hat{\Pi}_n^\perp) \hat{\mathcal{C}}(t) | \Psi_n \rangle \\ &\leq \langle \Psi_n | \hat{\mathcal{C}}^\dagger(t) \hat{\mathcal{C}}(t) | \Psi_n \rangle \leq \|\hat{\mathcal{C}}(t)\|^2, \end{aligned} \quad (9)$$

where $\hat{\Pi}_n^\perp$ projects onto the subspace orthogonal to that spanned by $|\Psi_n\rangle\langle\Psi_n|$ and $\|\hat{\mathcal{C}}\|^2$ is the operator norm. Substitution of this inequality into line (8) gives

$$\mathcal{I}_{rc}^{(q)} \leq 4 \|\hat{\mathcal{C}}(t)\|^2. \quad (10)$$

This is the central result of this work—the amount of information that can be extracted from the receiver is upper-bounded by the LRB. To estimate or measure the LRB it is thus sufficient to perform local single-body measurements. To recapitulate, this derivation does not rely on any assumptions about the input state $\hat{\rho}$, nor about the system, or the Hamiltonian \hat{H} . Only the initial transformation is assumed to be in the general form of Eq. (2) and the receiver to be a single qubit.

We now discuss the conditions under which this inequality can be saturated. The line (7) becomes an equality when the state $\hat{\rho}(\theta)$ is pure. The first inequality in line (9) is saturated when $|\Psi_n\rangle$ is an eigenstate of $\hat{\mathcal{C}}(t)$ and if the modulus of its eigenvalue is maximal, then this also saturates the last relation.

Finding the spectrum of $\hat{\mathcal{C}}(t)$ is usually hard. We show that the relation between the QFI and the LRB not only sheds some new light on both these quantities, but also allows to analytically derive the LRB using the knowledge of $\mathcal{I}_{rc}^{(q)}$. For illustration, we pick the XY spin chain depicted by the Hamiltonian

$$\hat{H} = \sum_i (\hat{\sigma}_i^{(x)} \hat{\sigma}_{i+1}^{(x)} + \hat{\sigma}_i^{(y)} \hat{\sigma}_{i+1}^{(y)}), \quad (11)$$

which is an excellent model for analysing the propagation of the signal through a system. The impulse acts on the source qubit, and its generator is one of the Pauli matrices, say $\hat{\sigma}_{sr}^{(x)}$. Subsequently, the Hamiltonian (11) propagates the signal to the receiver, positioned n qubits away from the source.

In order to saturate Eq. (10) we shall determine the maximal value of $\mathcal{I}_{rc}^{(q)}$. According to [21],

$$\mathcal{I}_{rc}^{(q)} \leq 4\Delta^2 \hat{h} = 4(\langle \hat{h}^2 \rangle - \langle \hat{h} \rangle^2), \quad (12)$$

where \hat{h} generates the infinitesimal transformation of $\hat{\rho}_{rc}^{(\theta)}(t)$ to $\hat{\rho}_{rc}^{(\theta+\delta\theta)}(t)$. The above inequality is saturated if $\hat{\rho}_{rc}^{(\theta)}(t) = |\psi_{rc}^{(\theta)}(t)\rangle\langle\psi_{rc}^{(\theta)}(t)|$, i.e., it is pure, and this happens when the input state $\hat{\rho} = |\psi\rangle\langle\psi|$ is the density operator representing, symmetrically, either of the two pure states

$$|\psi\rangle = |0, \dots, 0\rangle \equiv |\vec{0}\rangle, \quad \text{or} \quad |\psi\rangle = |1, \dots, 1\rangle \equiv |\vec{1}\rangle, \quad (13)$$

where $|0\rangle$ and $|1\rangle$ are the single-qubit eigenstates of $\hat{\sigma}^{(z)}$. These are the only states of zero eigenvalue of the Hamiltonian (11), yielding a non-entangled state at any time t . Other states will entangle, producing a mixed output at the receiver. We take one of the states from (13), for instance $|\psi\rangle = |\vec{0}\rangle$ as the input state and choose the

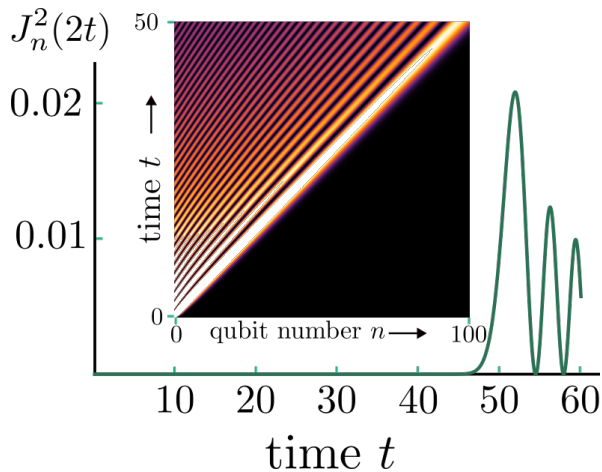


FIG. 2. The main figure shows the time-dependence of the Bessel function $J_n^2(2t)$ for $n = 100$. The inset is a space-time plot of $J_n^2(2t)$ ($n \in [0, 100]$ and $t \in [0, 50]$), showing the characteristic light cone-like structure.

working point $\theta = 0$ [38], giving, up to the dominant order (see Appendix),

$$|\psi_{rc}^{(\theta)}(t)\rangle = (\hat{\mathbb{1}} - i\theta J_n(2t)\hat{\sigma}_{rc}^{(x)})|0\rangle_{rc}, \quad (14)$$

where $J_n(2t)$ is the Bessel function of the first kind. Hence the generator of the transformation is $J_n(2t)\hat{\sigma}_{rc}^{(x)}$, and plugged into Eq. (12) gives

$$\mathcal{I}_{rc}^{(q)} \leq 4J_n(2t)^2, \quad (15)$$

which, according to Eq. (10), provides the LRB for this model. Note that once the relation (10) was established, the derivation of the LRB required only the knowledge of the properties of $\mathcal{I}_{rc}^{(q)}$. The Fig. 2 shows the dependence of $J_n^2(2t)$ on time for $n = 100$. The signal grows exponentially around $t = n/2 = 50$. Varying both n from 0 to 100 and t from 0 to 50 highlights the emblematic light cone-like structure with the speed of propagation, see Eq. (1), equal to $v = 2$.

We note that the QFI from Eq. (5) is the result of maximization of the Fisher information

$$\mathcal{I}_{rc} = \sum_x \frac{1}{p(x|\theta)} \left(\frac{\partial p(x|\theta)}{\partial \theta} \right)^2 \quad (16)$$

over all possible measurement operators $\hat{E}_{rc}(x)$ [21], where the probability of obtaining a result x is

$$p(x|\theta) = \text{Tr}[\hat{\rho}_{rc}^{(\theta)}(t)\hat{E}_{rc}(x)] \quad (17)$$

and $\sum_x \hat{E}_{rc}(x) = \hat{\mathbb{1}}$, $\hat{E}_{rc}(x) \geq 0$. While in general it is hard to determine the set of $\hat{E}_{rc}(x)$ for which the Fisher information from Eq. (16) saturates the QFI from Eq. (5), in the case of the Hamiltonian (11), according to Eq. (14) the probabilities of finding the receiver

qubit in states $|0\rangle_{rc}$ and $|1\rangle_{rc}$ around the working point $\theta = 0$, up to the leading order, are $p(0|\theta) \simeq (1 - \theta^2 J_n^2(2t))$ and $p(1|\theta) \simeq \theta^2 J_n^2(2t)$, which plugged into Eq. (16) gives $\mathcal{I}_{rc} = 4J_n^2(2t)$. Hence the simple single-qubit measurements allow to saturate the QFI bound and in consequence determine the LRB.

It is worth noting that the steps that are necessary to estimate the LRB have already been demonstrated experimentally in a different context. The small (quasi-infinitesimal) increments of θ were implemented experimentally in [23] for a similar purpose—to measure local properties of a probability and to estimate the value of the Fisher information a complex many-body system.

In conclusion, we have demonstrated that the Lieb-Robinson bound can be derived from local measurements on a single qubit connected to a many-body system, hence shifting the necessity of measuring correlation functions between distant subsystems. This is possible, because as we have shown, the LRB intrinsically limits the amount of information that reaches a single qubit that is a part of a complex many-body system. We have identified the conditions under which the local measurements on this qubit can saturate the upper limit set by the LRB, hence allowing one to determine the LRB from simple one-body measurements. We have used an example of the XY spin chain to show how the two formulations—that of the LRB and of quantum information—interplay, allowing to determine the velocity of information propagation. Due to the relative simplicity of the one-qubit operations and measurements, the protocol presented in this work might find applications in future measurements of the LRB, hence contributing to our understanding of complex many-body systems.

We acknowledge the discussion with Miłosz Panfil and Tomasz Wasak. This work was supported by the National Science Centre, Poland, within the QuantERA II Programme that has received funding from the European Union’s Horizon 2020 research and innovation programme under Grant Agreement No 101017733, Project No. 2021/03/Y/ST2/00195.

Appendix A: state evolution in XY model

The initial source state

$$|\psi\rangle = |0\rangle_{sr} \quad (A.1)$$

evolves under the local transformation $e^{-i\theta\hat{\sigma}_{sr}^{(x)}}$ to

$$|0\rangle_{sr} \longrightarrow \cos\theta|0\rangle_{sr} - i\sin\theta|1\rangle_{sr}. \quad (A.2)$$

Hence the state that undergoes the time evolution is (we label the source qubit with index 0 and use $\alpha = \cos\theta$, $\beta = -i\sin\theta$)

$$|\psi(\theta; t=0)\rangle = \alpha|\vec{0}\rangle + \beta|1\rangle_0 \bigotimes_{\kappa \neq 0} |0\rangle_{\kappa}, \quad (A.3)$$

and it is propagated with the Hamiltonian from Eq. (11). The first part, $|\vec{0}\rangle$, does not evolve under the Hamiltonian (11) (it is its eigenstate with zero eigenvalue), while the evolution of the second, i.e.,

$$|\phi\rangle = |1\rangle_0 \bigotimes_{\kappa \neq 0} |0\rangle_\kappa \quad (\text{A.4})$$

can be found using the Taylor series of the evolution operator. The one-fold action of \hat{H} on the state gives

$$\hat{H}|\phi\rangle = |1\rangle_1 \bigotimes_{\kappa \neq 1} |0\rangle_\kappa + |1\rangle_{-1} \bigotimes_{\kappa \neq -1} |0\rangle_\kappa. \quad (\text{A.5})$$

Both the components of the resulting state have the same form as the initial one, but now the excitations have moved to the adjacent qubits. Another action of the Hamiltonian yields

$$\hat{H}^2|\phi\rangle = |1\rangle_2 \bigotimes_{\kappa \neq 2} |0\rangle_\kappa + 2|1\rangle_0 \bigotimes_{\kappa \neq 0} |0\rangle_\kappa + |1\rangle_{-2} \bigotimes_{\kappa \neq -2} |0\rangle_\kappa. \quad (\text{A.6})$$

In general, the μ -fold action will give the coefficients of the Newton binomial and the excitation of odd/even kets, depending on the parity of μ .

Thus the state will take the form

$$\hat{H}^\mu|\phi\rangle = \sum_{\nu=0}^{\mu} \binom{\mu}{\nu} |1\rangle_{\kappa_\nu} \bigotimes_{\kappa \neq \kappa_\nu} |0\rangle_\kappa, \quad (\text{A.7})$$

where $\kappa_\nu = 2\nu - \mu$. The full state at time t is

$$|\psi(\theta; t)\rangle = \alpha|\vec{0}\rangle + \beta \sum_{\mu=1}^{\infty} \frac{(-it)^\mu}{\mu!} \sum_{\nu=0}^{\mu} \binom{\mu}{\nu} |1\rangle_{\kappa_\nu} \bigotimes_{\kappa \neq \kappa_\nu} |0\rangle_\kappa. \quad (\text{A.8})$$

The density matrix for this pure state is

$$\hat{\rho}(\theta; t) = |\psi(\theta; t)\rangle\langle\psi(\theta; t)| \quad (\text{A.9})$$

and according to Eq. (4), the state of the receiver is obtained by tracing out the non-receiver degrees of freedom, i.e.,

$$\hat{\rho}_{rc}^{(\theta)}(t) = \widetilde{\text{Tr}}[\hat{\rho}(\theta; t)]. \quad (\text{A.10})$$

After some algebraic manipulations we obtain

$$\begin{aligned} \hat{\rho}_{rc}^{(\theta)} &= |0\rangle\langle 0|_{rc} (1 - |\beta|^2 J_n^2(2t)) \\ &+ \alpha J_n(2t) (|0\rangle\langle 1|_{rc} \beta + |1\rangle\langle 0|_{rc} \beta^*) \\ &+ |\beta|^2 J_n^2(2t) |1\rangle\langle 1|_{rc}. \end{aligned} \quad (\text{A.11})$$

The dominant eigenvalue is shown in Fig. 3 using exemplary values of $n = 100$ and $t = 52$. The state is pure only for $\theta = 0$. Expanding for small θ around 0 we obtain

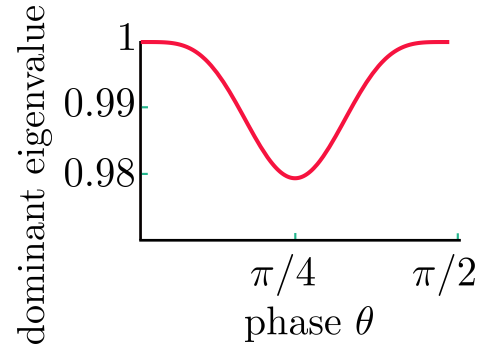


FIG. 3. The dominant eigenvalue of the receiver density matrix from Eq. (A.11) with $n = 100$ and $t = 52$.

$$\begin{aligned} \hat{\rho}_{rc}^{(\theta)} &= |0\rangle\langle 0|_{rc} (1 - \theta^2 J_n^2(2t)) \\ &+ i\theta J_n(2t) (|0\rangle\langle 1|_{rc} - |1\rangle\langle 0|_{rc}) \\ &+ \theta^2 J_n^2(2t) |1\rangle\langle 1|_{rc}, \end{aligned} \quad (\text{A.12})$$

which is, up to the dominant terms in small θ , the density matrix of the pure state from Eq. (14) reported in the main text.

-
- [1] E. H. Lieb and D. W. Robinson, The Finite Group Velocity of Quantum Spin Systems, *Comm. Math. Phys.* **28**, 251 (1972).
 - [2] I. Prémont-Schwarz and J. Hnybida, Lieb-Robinson Bounds on the Speed of Information Propagation, *Phys. Rev. A* **81**, 062107 (2010).
 - [3] D. A. Roberts and B. Swingle, Lieb-Robinson Bound and the Butterfly Effect in Quantum Field Theories, *Phys. Rev. Lett.* **117**, 091602 (2016).
 - [4] M. C. Tran, A. Y. Guo, C. L. Baldwin, A. Ehrenberg, A. V. Gorshkov, and A. Lucas, Lieb-Robinson Light Cone for Power-Law Interactions, *Phys. Rev. Lett.* **127**, 160401 (2021).
 - [5] S. Bravyi, M. B. Hastings, and F. Verstraete, Lieb-Robinson Bounds and the Generation of Correlations and Topological Quantum Order, *Phys. Rev. Lett.* **97**, 050401 (2006).
 - [6] M. P. Fisher, V. Khemani, A. Nahum, and S. Vijay, Random Quantum Circuits, *Annual Review of Condensed Matter Physics* **14**, 335 (2023).
 - [7] M. Gebert and M. Lemm, On Polynomial Lieb-Robinson Bounds for the XY Chain in a Decaying Random Field, *J. Stat. Phys.* **164**, 667 (2016).
 - [8] D. V. Else, F. Machado, C. Nayak, and N. Y. Yao, Improved Lieb-Robinson Bound for Many-Body Hamiltonians with Power-Law Interactions, *Phys. Rev. A* **101**, 022333 (2020).
 - [9] N. Shiraishi and H. Tajima, Efficiency Versus Speed in Quantum Heat Engines: Rigorous Constraint from Lieb-Robinson Bound, *Phys. Rev. E* **96**, 022138 (2017).
 - [10] Z. Wang and K. R. Hazzard, Tightening the Lieb-Robinson Bound in Locally Interacting Systems, *PRX Quantum* **1**, 010303 (2020).
 - [11] H. Wilming and A. H. Werner, Lieb-Robinson Bounds

- Imply Locality of Interactions, *Phys. Rev. B* **105**, 125101 (2022).
- [12] D. Poulin, Lieb-Robinson Bound and Locality for General Markovian Quantum Dynamics, *Phys. Rev. Lett.* **104**, 190401 (2010).
- [13] J. Jünemann, A. Cadarso, D. Pérez-García, A. Bermudez, and J. J. García-Ripoll, Lieb-Robinson Bounds for Spin-Boson Lattice Models and Trapped Ions, *Phys. Rev. Lett.* **111**, 230404 (2013).
- [14] P. Hauke and L. Tagliacozzo, Spread of Correlations in Long-Range Interacting Quantum Systems, *Phys. Rev. Lett.* **111**, 207202 (2013).
- [15] B. Nachtergaele, Y. Ogata, and R. Sims, Propagation of Correlations in Quantum Lattice Systems, *J. Stat. Phys.* **124**, 1 (2006).
- [16] J. Faupin, M. Lemm, and I. M. Sigal, On Lieb-Robinson Bounds for the Bose-Hubbard Model, *Comm. Math. Phys.* **394**, 1011 (2022).
- [17] B. J. Mahoney and C. S. Lent, The Lieb-Robinson Correlation Function for the Quantum Transverse Field Ising Model, arXiv:2402.11080.
- [18] M. Cheneau, P. Barmettler, D. Poletti, M. Endres, P. Schauß, T. Fukuhara, C. Gross, I. Bloch, C. Kolthath, and S. Kuhr, Light-Cone-Like Spreading of Correlations in a Quantum Many-Body System, *Nature* **481**, 484 (2012).
- [19] Y. Chu, X. Li, and J. Cai, Strong Quantum Metrological Limit from Many-Body Physics, *Phys. Rev. Lett.* **130**, 170801 (2023).
- [20] H.-L. Shi, X.-W. Guan, and J. Yang, Universal Shot-Noise Limit for Quantum Metrology with Local Hamiltonians, *Phys. Rev. Lett.* **132**, 100803 (2024).
- [21] S. L. Braunstein and C. M. Caves, Statistical Distance and the Geometry of Quantum States, *Phys. Rev. Lett.* **72**, 3439 (1994).
- [22] L. Pezzé and A. Smerzi, Entanglement, Nonlinear Dynamics, and the Heisenberg Limit, *Phys. Rev. Lett.* **102**, 100401 (2009).
- [23] P. Hyllus, W. Laskowski, R. Krischek, C. Schwemmer, W. Wieczorek, H. Weinfurter, L. Pezzé, and A. Smerzi, Fisher Information and Multiparticle Entanglement, *Phys. Rev. A* **85**, 022321 (2012).
- [24] G. Tóth, Multipartite Entanglement and High-Precision Metrology, *Phys. Rev. A* **85**, 022322 (2012).
- [25] P. Hauke, M. Heyl, L. Tagliacozzo, and P. Zoller, Measuring Multipartite Entanglement Through Dynamic Susceptibilities, *Nat. Phys.* **12**, 778 (2016).
- [26] B. Yadin, M. Fadel, and M. Gessner, Metrological Complementarity Reveals the Einstein-Podolsky-Rosen Paradox, *Nat. Comm.* **12**, 2410 (2021).
- [27] A. Niezgoda and J. Chwedeńczuk, Many-Body Nonlocality as a Resource for Quantum-Enhanced Metrology, *Phys. Rev. Lett.* **126**, 210506 (2021).
- [28] M. Prokopenko, J. T. Lizier, O. Obst, and X. R. Wang, Relating Fisher Information to Order Parameters, *Phys. Rev. E* **84**, 041116 (2011).
- [29] T.-L. Wang, L.-N. Wu, W. Yang, G.-R. Jin, N. Lambert, and F. Nori, Quantum Fisher Information as a Signature of the Superradiant Quantum Phase Transition, *New J. Phys.* **16**, 063039 (2014).
- [30] U. Marzolino and T. c. v. Prosen, Fisher Information Approach to Nonequilibrium Phase Transitions in a Quantum XXZ Spin Chain with Boundary Noise, *Phys. Rev. B* **96**, 104402 (2017).
- [31] J. Ma and X. Wang, Fisher Information and Spin Squeezing in the Lipkin-Meshkov-Glick Model, *Phys. Rev. A* **80**, 012318 (2009).
- [32] C. Invernizzi, M. Korbman, L. Campos Venuti, and M. G. A. Paris, Optimal Quantum Estimation in Spin Systems at Criticality, *Phys. Rev. A* **78**, 042106 (2008).
- [33] P. Zanardi, M. G. A. Paris, and L. Campos Venuti, Quantum Criticality as a Resource for Quantum Estimation, *Phys. Rev. A* **78**, 042105 (2008).
- [34] G. Salvatori, A. Mandarino, and M. G. A. Paris, Quantum Metrology in Lipkin-Meshkov-Glick Critical Systems, *Phys. Rev. A* **90**, 022111 (2014).
- [35] M. Bina, I. Amelio, and M. G. A. Paris, Dicke Coupling by Feasible Local Measurements at the Superradiant Quantum Phase Transition, *Phys. Rev. E* **93**, 052118 (2016).
- [36] L. Garbe, M. Bina, A. Keller, M. G. A. Paris, and S. Felicetti, Critical Quantum Metrology with a Finite-Component Quantum Phase Transition, *Phys. Rev. Lett.* **124**, 120504 (2020).
- [37] A. Piga, A. Aloy, M. Lewenstein, and I. Frérot, Bell Correlations at Ising Quantum Critical Points, *Phys. Rev. Lett.* **123**, 170604 (2019).
- [38] For all other θ 's the input state must be of the form $|\psi\rangle = e^{i\theta h}|\vec{0}\rangle$ or $|\psi\rangle = e^{i\theta h}|\vec{1}\rangle$ to accommodate for the shift of the working point.